Understanding α,β-Unsaturated Imine Formation from Amine Additions to α,β-Unsaturated Aldehydes and Ketones – An Analytical and Theoretical Investigation.

Adam D. J. Calow,[†] Jorge J. Carbó,[*‡] Jessica Cid,[‡] Elena Fernández[‡] and Andrew Whiting.[*†]

[†]A. D. J. Calow & Dr A. Whiting, Centre for Sustainable Chemical Processes, Department of Chemistry, Science Laboratories, Durham University, South Road, Durham, DH1 3LE (UK), E-mail: andy.whiting@durham.ac.uk

[‡]Dr J. J. Carbó, Dr J. Cid & Dr E. Fernández, Departament Química Física I Inorgànica, University Rovira I Virgili, C/Marcel.lí Domingo s/n 43007, Tarragona (Spain).

Abstract

A combination of *in situ* IR spectroscopy (ReactIR^{TM}) and DFT calculations have been used to understand what factors govern the selectivity in the addition of primary amines to α,β-unsaturated aldehydes and ketones, *i.e.* 1,2- *vs*. 1,4-addition. It has been found that the 1,2-addition products (α,β-unsaturated imines following addition-elimination) usually predominate for most systems. However, exceptions, such as methyl vinyl ketone, selectively give 1,4-addition products. This has been rationalized by DFT calculations which show that major conformational effects are involved, controlled mainly by steric effects of carbonyl substituents, resulting in a model which provides simple and predictable preparation of α,β-unsaturated imines for generation *in situ* utilization in synthesis.

Introduction

The addition of nucleophiles to conjugated electron-deficient alkenes (*e.g.* α,β-unsaturated aldehydes, amides, esters and ketones) is one of the most important C-C and C-heteroatom

bond forming reactions in organic synthesis.[1] However, due to the possibility of conjugate (1,4-) *vs.* direct (1,2-) addition, a thorough understanding of the factors that govern these competing pathways is required.

We recently developed catalytic asymmetric routes to chiral γ-amino alcohols[2] (Scheme 1), whereby α,β-unsaturated imines **3** were utilized as starting materials by generation *in situ*. The *in situ* generation was absolutely essential to allow this methodology to work on a range of substrates and to give clean products and in good yields. However, in the process of preparing these α,β-unsaturated imines **3**,[2] we discovered a lack of kinetic or mechanistic studies regarding the relative 1,2- *vs.* 1,4-addition of primary amines **2** to α,β-unsaturated aldehydes and ketones **1** (enals and enones, respectively). This is surprising given the wealth of studies examining both the aza-Michael[3] reaction and that of classical imine formation (from aldehydes and ketones).[4] Nevertheless, other groups have utilized such imines **3** in synthesis[5-8] and have reported their preparation *via* aza-Wittig chemistry,[9] simple condensation and catalytic methods.[10] Herein, we report the use of a combination of *in situ* IR spectroscopy (ReactIR^{TM})[11] backed up by NMR studies, and DFT calculations, with the aim of understanding the addition of primary amines **2** to α,β-unsaturated aldehydes and ketones **1** (1,2- *vs.* 1,4-addition) and examine the relative rates of these reactions. Furthermore, we show which 1,2-addition products (*i.e.* α,β-unsaturated imines **3** following the addition-elimination process**)** are generated cleanly, and in such a way that they can be utilized in synthesis without the need for isolation. This procedure therefore makes a number of α,β-unsaturated imines readily available in an efficient and atom-economic way for further synthetic applications (see Scheme 1).

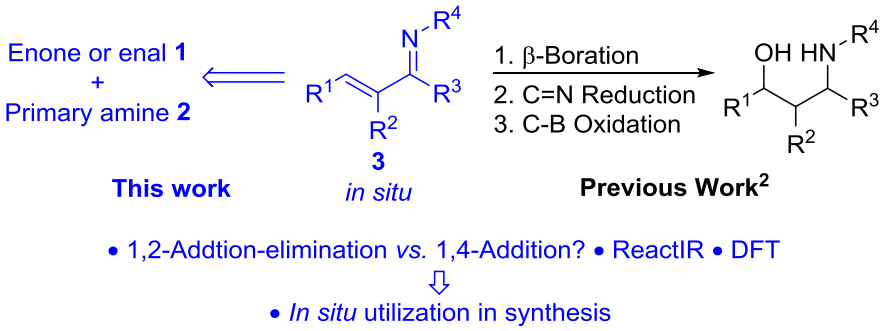

Scheme 1 *In situ* generated α,β-unsaturated imines: ideal for various one-pot formation-functionalization sequences.

Results and Discussion

In Situ IR Spectroscopy Study

Initially, we suspected that the addition of a primary amines **2** (R^4-NH_2, where R^4 = alkyl or aryl) to enals or enones **1** resulted in mixtures of 1,2- and 1,4-addition products (*i.e.* **3** and **4**, respectively). It is typically considered that 1,2-addition products are kinetically preferred and that the 1,4-addition products are thermodynamically preferred due to the reversibility of the 1,2-addition step *via* facile imine hydrolysis and hemi-aminal intermediates.[12] Hence, we initially decided to investigate the addition of benzylamine ($BnNH_2$) **2a** to crotonaldehyde **1a**, methacrolein **1b** and methyl vinyl ketone **1c**, both with and without 3 Å-molecular sieves (3 Å-MSs) as drying agent at room temperature (see Table 1).

To our surprise, we observed either exclusive 1,2- (entries 1 to 4, Table 1) or 1,4-addition (entries 4 and 5, Table 1) irrespective of whether 3 Å-MSs were present in the reaction mixture or not. However, it should be noted that in the case of methacrolein **1b**, the reaction time was longer when compared to the reaction where 3 Å-MSs were employed (the role of the molecular sieves will be discussed later, *vide infra*), and leading to the 1,2-addition product as clearly demonstrated by ReactIR (see Figures 1a-c for typical ReactIR data). More importantly however, was the observation that seemingly no 1,4-addition products formed.

1,2-Addition could be clearly deduced (as shown by Figures 1a-c) since the reaction profiles clearly showed the loss of the C=O absorption at 1703 cm^{-1} for methacrolein **1b**, and the concomitant appearance of **3ba** shown graphically by the C=N absorption at 1622 cm^{-1}. Figure 1b shows the IR-spectrum between 1820-1580 cm^{-1} region for the reaction of methacrolein **1b** with $BnNH_2$ **2a**, and overlay of three spectra at different time intervals (t = 0, 10 and 80 min). This shows that there is total loss of the starting C=O stretch and that this is synchronized with the rise of the C=N (both asymmetric and symmetric) stretches and importantly, there is no observable 1,4-addition product at higher wavenumbers. Finally, Figure 1c shows the ReactIR output, showing the intensity of the stretch (arbitrary units, AU) *vs.* wavenumber (cm^{-1}) over time.

Table 1 1,2- or 1,4-Addition of $BnNH_2$ to crotonaldehyde **1a**, methacrolein **1b** and methyl vinyl ketone **1c**.

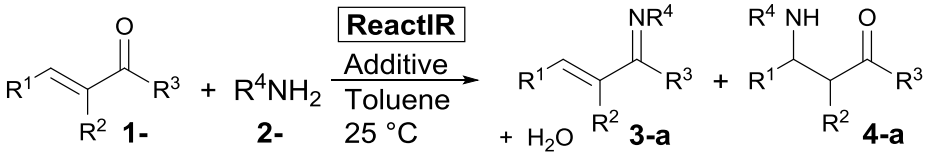

Entry	Substrate **1-**	Additive	Primary Product	Time, t (min)	$I_{C=O\ 1/2}$ (min)
1[a]	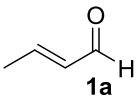 **1a**	3 Å-MS	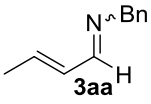 **3aa**	135	5
2		-		176	5
3[a]	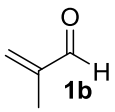 **1b**	3 Å-MS	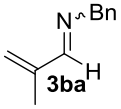 **3ba**	80	11
4		-		444	85
5[a]	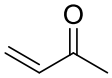 **1c**	3 Å-MS	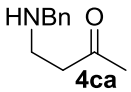 **4ca**	85	6
6		-		82	14

Conditions: Enone/enal **1** (2.0 mmol) added to a stirred mixture of toluene (8 mL) and 3 Å-MSs (oven-dried at 250 ºC for >48 h) at 25 ºC. Amine (2.0 mmol) added and monitored by ReactIR™. [a]3 Å-MSs oven-dried at 250 ºC for >48 h prior to use.

Interestingly, in the case of methyl vinyl ketone **1c**, no 1,2-addition product **3** was observed (Table 1, entries 5 and 6), only 1,4-addition took place, as shown in Figures 2a-b, even when 3Å-MSs were employed. This suggests that 1,4-addition product **4** is kinetically preferred by ketone **1c**. An alternative explanation is that there is a facile, and rapid hydrolysis, of the imine (by the water generated from the condensation), thus releasing the amine **2a** to proceed to do the 1,4-addition, *i.e.* under thermodynamic control. However, this is unlikely given that an imine intermediate was not observed in the case of reaction of **1a** and **1b** especially when no 3 Å-MSs were used. This is particularly clear from ReactIR studies, as shown in Figure 2a, which shows the rapid loss of the carbonyl stretch of **1c** (*i.e.* C=O stretch at 1686 cm^{-1}) and the concomitant gain of the secondary amine functionality of **4ca** at higher wavelength (1719 cm^{-1}). The 1,4-Addition product **4ca** was also found to be consumed after 30 minutes, which is likely due to addition of the secondary amine **4ca** to further unsaturated ketone **1c**, which is demonstrated by the loss of the C=O stretch at 1719 cm^{-1}. Indeed, when studied in parallel with the ReactIR (Figure 2b), further 1,4-addition is clearly observed by the appearance of the C=O stretch at higher wavelength (1719 cm^{-1}).

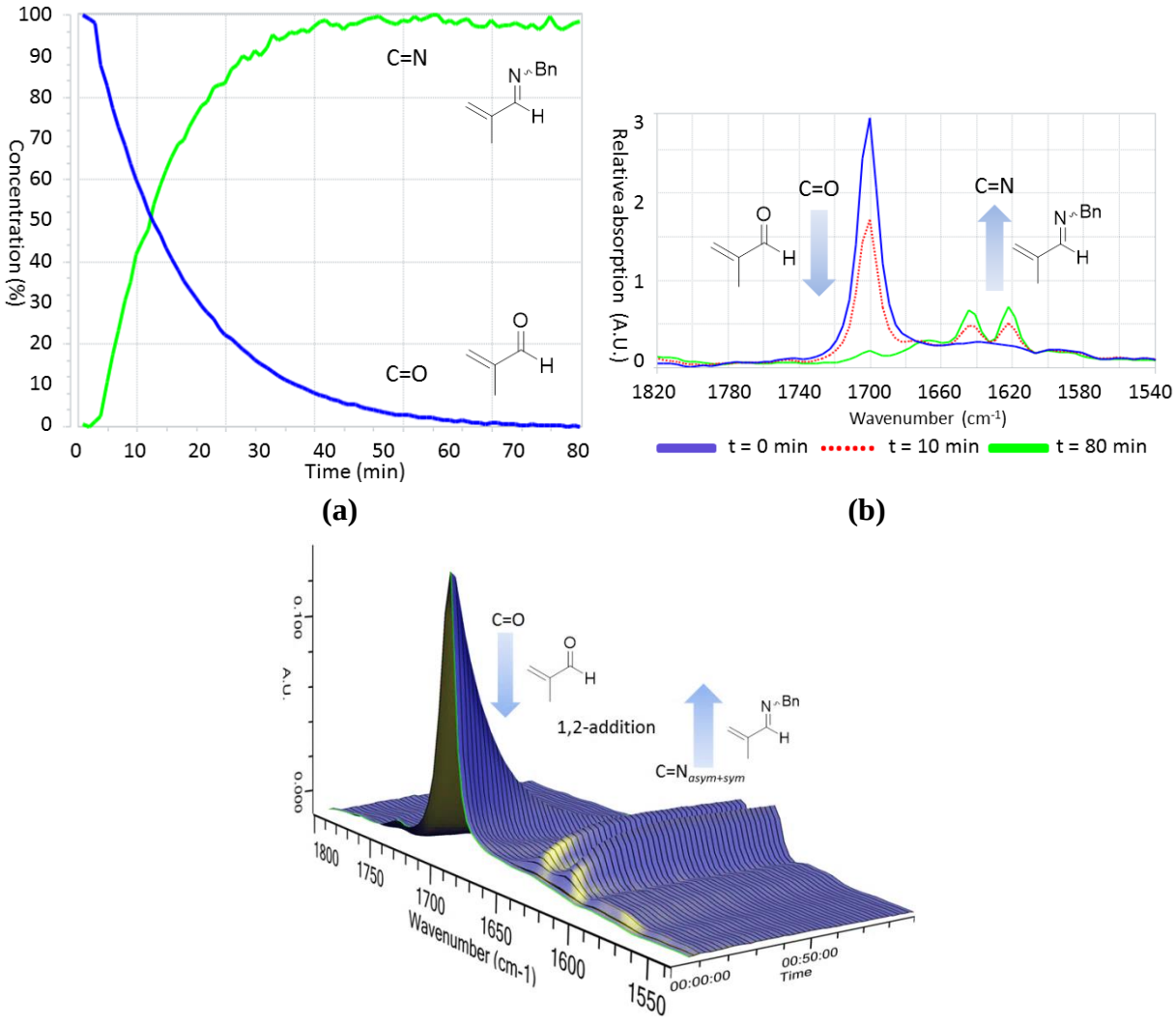

Figure 1. Data from entry 3, Table 1: a) Reaction profile showing the loss of **1b** (1703 cm^{-1}) and the concomitant gain of **3ba** (1622 cm^{-1}) - 1,2-addtion; b) Superimposed IR spectra at t = 0, t = 10 and t = 80 min, showing the loss of C=O **1b** (1703 cm^{-1}) and gain of the $C=N_{asym + sym}$ stretches for **3ba** (at 1640 and 1622 cm^{-1}, respectively). c) ReactIR showing the reaction profile over time (1 sample min^{-1}).

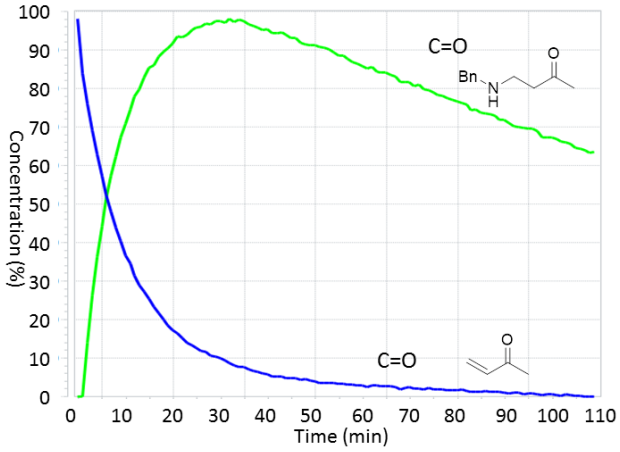

(a)

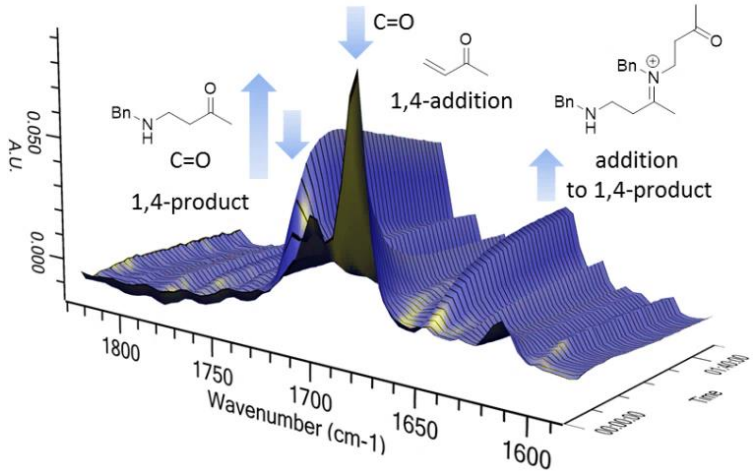

(b)

Figure 2. Data from Entry 5, Table 1: a) Reaction profile showing the rapid loss of **1c** (1686 cm^{-1}) and the concomitant gain of **4ca** (1719 cm^{-1}), followed by the loss of **4ca** (1719 cm^{-1}) - consistent with 1,4-addition, with further self-addition of species **4ca**; b) ReactIR graphical output showing the reaction profile over time (1 sample min^{-1}).

In order to validate the ReactIR results shown in Table 1, we carried out parallel *in situ* NMR experiments in d_8-toluene for the reactions between crotonaldehyde **1a**, methacrolein **1b** and methyl vinyl ketone **1c** with benzylamine **2a**, both with and without 3 Å-MSs. Some of these results are shown in Table 2 and Figure 3a-c, which portray results which are complimentary to those reported Table 1 and Figures 1a-c and 2a-b (additional experimental data are reported in the ESI).

Table 2 ^{1}H-NMR study of imine formation between carbonyl compounds **1-** and benzylamine **2a** for comparison with the results reported in Table 1.

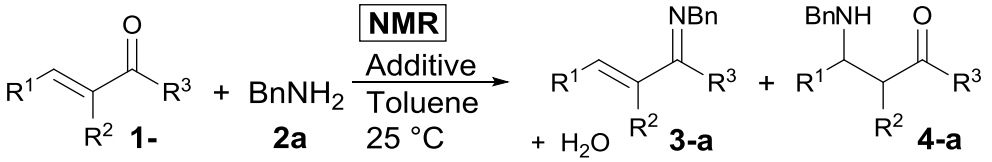

Entry	Substrate **1-**	Additive	Time (min)	Conversion (%) **3-a**	**4-a**
1	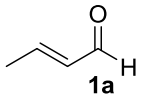 **1a**	3 Å-MS	310	**3aa** (90)	0
2		-	360	**3aa** (90)	0
3	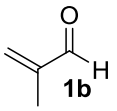 **1b**	3 Å-MS	1320	**3ba** (86)	0
4		-	1320	**3ba** (67)	0
5	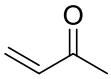 **1c**	3 Å-MS	140	0	**4ca** (>99)
6		-	140	0	**4ca** (>99)

Enal or enone **1** (0.18 mmol) added to NMR tube (Norell® Standard Series™ 5 mm x 178 mm NMR tubes) in d_8-toluene (0.7 mL) with & without 3 Å-MS beads (filled 0.7-0.8 mm up the tube, MS beads oven-dried at 250 ºC for >48 h prior to use), flushed with Ar and sealed. After acquisition of the first spectrum, amine **2** (0.18 mmol) added and next spectrum acquired in <5 min. Subsequent ^{1}H-NMR spectra were recorded over time with intermittent shaking to aid mixing.

The results shown in Table 2 broadly corroborate the findings obtained from the ReactIR studies (*vide supra*). Some enones, such as methyl vinyl ketone **1c**, undergo exclusive 1,4-addtion with primary amines, indicating that the 1,4-addition pathway is kinetic preferred. In contrast, methacrolein and crotonaldehyde undergo exclusive 1,2-addition, suggesting that in these cases the kinetic preference is for the 1,2-additon route. Moreover, the presence of 3 Å-MSs does not change the reaction outcome, however, in some cases the presence of 3 Å-MSs appears to drive the reaction closer to completion, as one might expect, presumably due to the removal of water pushing the condensation equilibrium. This is exemplified by methacrolein **1b** (see Entries 3 and 4, Table 2).

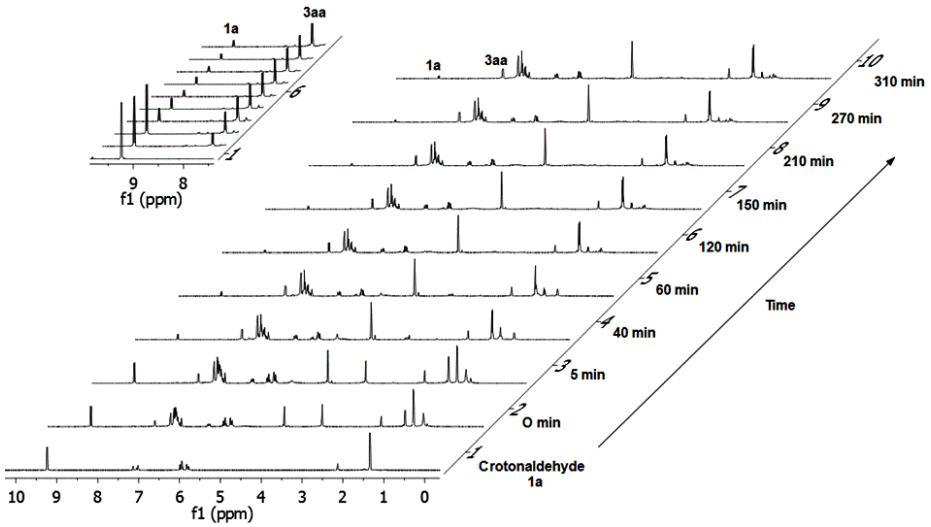

(a)

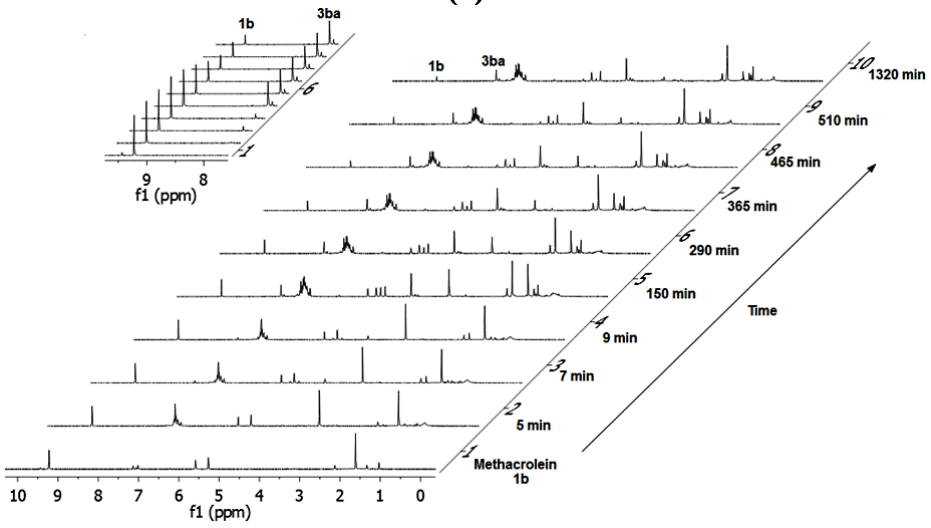

(b)

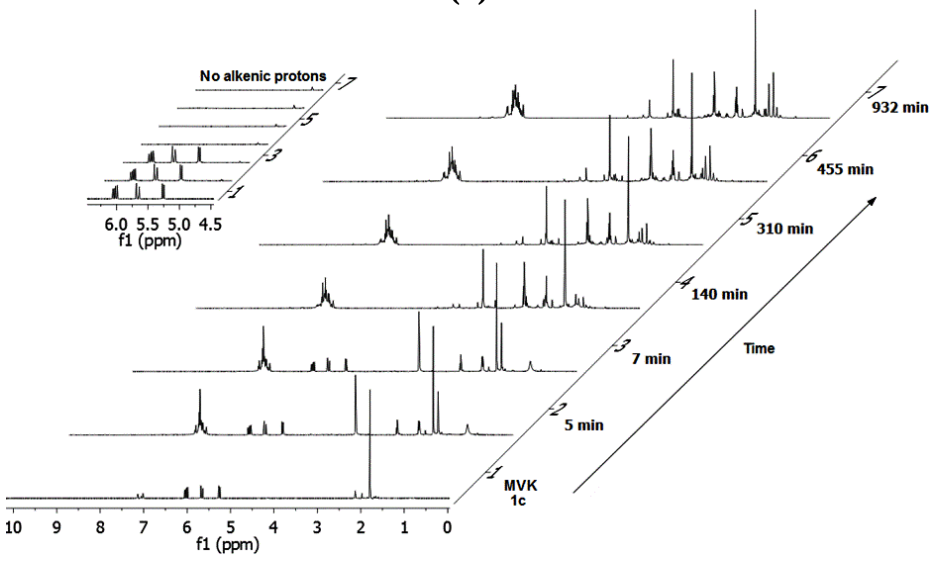

(c)

Figure 3 Real-time ^{1}H-NMR experiments showing the reaction between **1a**, **2a** and **3a** with **2a**, as shown in Table 2: (a) Entry 1; (b) Entry 3; (c) Entry 5.

It should be noted that the reactions appear slightly longer when carried under the NMR

experimental conditions compared to those employed for the ReactIR experiments. This can be exemplified by comparing the reaction of crotonaldehyde **1a** and benzylamine **2a** in the presence of 3 Å-MSs. When monitored by ReactIR, the reaction takes approximately 2.3 hours (Entry 1, Table 1), whereas in the NMR tube the reaction takes 5.2 hours (Entry 1, Table 2) to proceed to near completion. This is useful to know especially in the context of our past experience with using such *in situ*-generated imines directly for further reaction,[2] and is likely due to the different mixing (mass transfer) in the NMR tube compared to an efficiently stirred flask used for the ReactIR experiments. In fact, this is an additional advantage of ReactIR to follow such reactions over NMR because it can be carried out directly in the same reaction vessel one would use for further reactions, and on any desired scale.

Next, the role of the amine **2** and solvent on the selectivity and rates of reaction with the three previously investigated carbonyl compounds (**1a-c**) were investigated using benzylamine **2a**, aniline **2b** and *n*-butylamine **2c** in a non-polar (toluene) and polar (acetonitrile) solvent, as outlined in Tables 3 and 4.

From Tables 3 and 4, the first thing to note is that all the reactions proceeded to completion in <24 h when the reactions were carried out in toluene, whereas in acetonitrile, some reactions took >24 h (*i.e.* when using $PhNH_2$ **2b**). However, irrespective of whether the solvent was non-polar (toluene) or polar (acetonitrile), the reactions proceeded to give the same selectivity as one would expect from Table 1, *i.e.* **1a** and **1b** undergo 1,2-addition irrespective of the amine, and **1c** reacts exclusively in a 1,4-fashion with all the amines. In particular, the reaction between $PhNH_2$ **2b** and crotonaldehyde **1a** is particularly interesting due to the rapid consumption of the carbonyl compound **1a** and the formation of imine **3ab**. Further, the C=O peak intensity dropped 50% after only 9 minutes (Entry 1, Table 3), yet the reaction did not go to completion until approximately 6 h later (see Figure 4), which suggest

that reaction involves rapid hemi-aminal formation, followed by a slower dehydration to provide the imine (*vide infra*).

Table 3 Probing the effects of amine nucleophilicity in toluene.

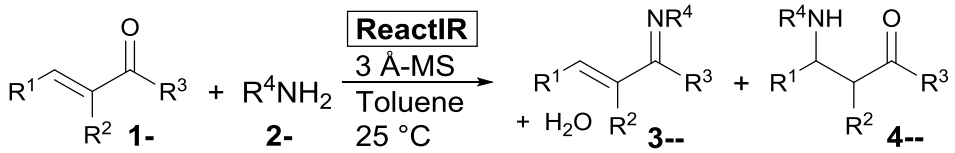

Entry	Substrate **1-**	Amine **2-**	Primary Product	Time, t (min)	$I_{C=O\ 1/2}$ (min)
1	**1a**	$PhNH_2$ **2b**	**3ab**	365	9
2	**1a**	$BnNH_2$ **2a**	**3aa**	135	5
3	**1a**	*n*$BuNH_2$ **2c**	**3ac**	96	5
4	**1b**	$PhNH_2$ **2b**	**3bb**	632	16
5	**1b**	$BnNH_2$ **2a**	**3ba**	80	11
6	**1b**	*n*$BuNH_2$ **2c**	**3ba**	87	10
7	**1c**	$PhNH_2$ **2b**	**4cb**	601	50
8	**1c**	$BnNH_2$ **2a**	**4ca**	85	6
9	**1c**	*n*$BuNH_2$ **2c**	**4cc**	55	3

Standard conditions as reported in Table 1.

Table 4 Probing the effects of amine nucleophilicity in acetonitrile.

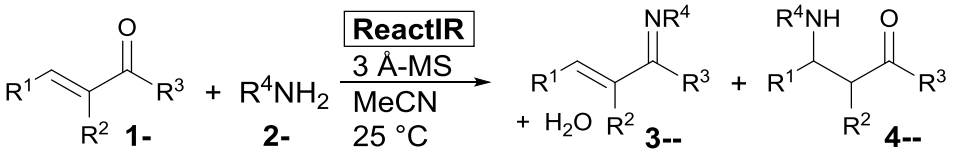

Entry	Substrate **1-**	Amine **2-**	Primary Product	Time, t (min)	$I_{C=O\ 1/2}$ (min)
1	**1a**	$PhNH_2$ **2b**	**3ab**	>1440	57
2	**1a**	$BnNH_2$ **2a**	**3aa**	178	5
3	**1a**	*n*$BuNH_2$ **2c**	**3ac**	296	4
4	**1b**	$PhNH_2$ **2b**	**3bb**	>1440	42
5	**1b**	$BnNH_2$ **2a**	**3ba**	174	14
6	**1b**	*n*$BuNH_2$ **2c**	**3ba**	145	12
7	**1c**	$PhNH_2$ **2b**	**4cb**	>1440	474
8	**1c**	$BnNH_2$ **2a**	**4ca**	84	9
9	**1c**	*n*$BuNH_2$ **2c**	**4cc**	46	3

Standard conditions (except where acetonitrile was used) as reported in Table 1.

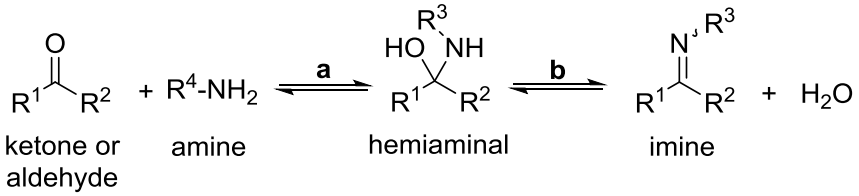

Scheme 2 Steps involved in imine formation.

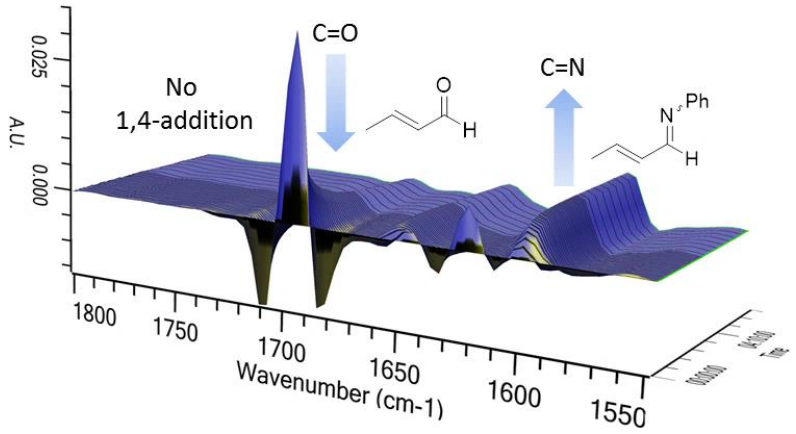

Figure 4 Graphical output of Entry 1, Table 3 showing the rapid loss of the C=O stretch for **1a** and the rise of the C=N stretch of **3ab** on addition of the soft nucleophile **2b**. Processing - 2nd derivative base-line function is applied.

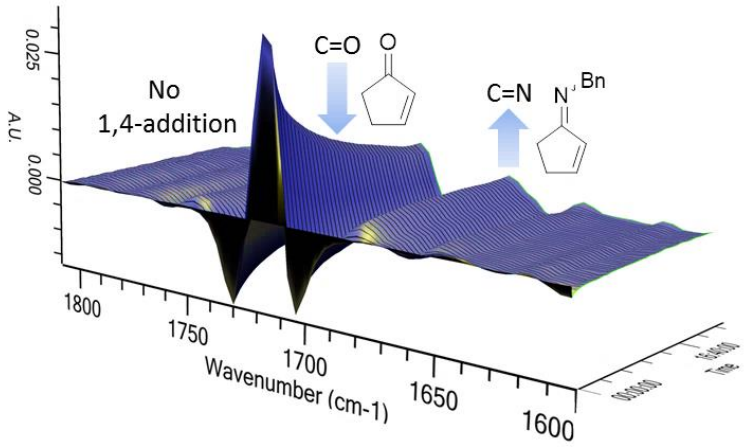

Figure 5 Graphical output of Entry 2, Table 5. Addition of **2a** to **1d** results in the slow formation of **3da**, but no 1,4-addition products are observed. Processing - 2nd derivative base-line function is applied.

Furthermore, imine formation appears to mirror the loss of the enal/enone, suggesting that the rate determining step is the addition of the amine, and not the collapse of the hemi-aminal intermediate (Scheme 2), as determined *in situ* IR spectroscopy. This is consistent with previous kinetic studies on imine formation in weakly acidic (3 Å-MSs) to neutral media.[13] Indeed, when such reactions are performed at acidic pH, the rate limiting step was found to be the addition of the amine to the corresponding carbonyl, due to competing amine protonation under the acidic conditions.[4] Moreover, acidic conditions assist dehydration of

the hemi-aminal intermediate and formation of the imine. In contrast, at basic pH, the rate determining step switched to collapse of the hemi-aminal intermediate.[13]

Next, three cyclic enones cyclopentenone **1d**, cyclohexenone **1e** and 3-methyl-2-cyclohexenone **1f** were examined in their reaction with $BnNH_2$ **2a** and $PhNH_2$ **2b** in toluene (see Table 5). It was assumed, given the exclusive 1,4-addition observed in the case of **1c** and that the increased ring strain of the α,β-unsaturated conjugated system results in the same 1,4-addition pathway as that observed with methyl vinyl ketone **1c**. However, to our surprise, 1,2-addition was observed in all cases, though these reactions required >24 h to go to completion. The C=O stretch intensities dropped to 50% (for both cyclopentenone and cyclohexenone) again surprisingly quickly, given the relatively long reaction times, especially in the cases involving the reaction with $BnNH_2$ **2a** (see Figure 5). In particular, 3-methyl-2-cyclohexeonone was significantly less reactive with the reaction only reaching 35% conversion to the α,β-unsaturated imine after 24 h (see ESI for IR spectral and *in situ* NMR validation for species **1d**).

Table 5 Cyclic enones: 1,2- *versus* 1,4-addition with primary amines.

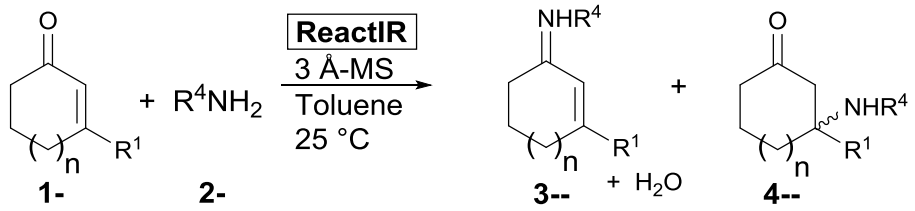

1- 2- 3-- 4--

Entry	Substrate **1-**	Amine **2-**	Primary Product	Time, t (h)	$I_{C=O\ 1/2}$ (h)
1	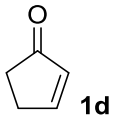 **1d**	$PhNH_2$ **2b**	**3db**	>24	17.4
2		$BnNH_2$ **2a**	**3da**	>24	4.0
3	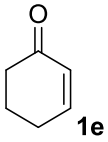 **1e**	$PhNH_2$ **2b**	**3eb**	>>24	7.4
4		$BnNH_2$ **2a**	**3ea**	>24	3.5
5	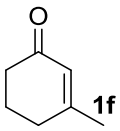 **1f**	$PhNH_2$ **2b**	**3fb**	>>24	-[a]
6		$BnNH_2$ **2a**	**3fa**	>24	18.8

Conditions: Enone 1 (2.0 mmol) was added to a stirring solution of toluene (8 mL) and 3 Å-MS (oven-dried at 250 ºC for >48 h prior to use). Amine (2.0 mmol) was added and the reaction monitored by ReactIR™. Reaction vessel was submerged in an oil bath and the temperature was maintained at 25 ºC. [a] Peak intensity = 35% after 24 h.

We continued our investigation by examining other acyclic enones and enals, looking at the effects of substituents on the C=C (*i.e.* α,β-di-substituted enals *vs.* β-substituted enals). Hence, cinnamaldehyde **1g** and α-methyl-cinnamaldehyde **1h**, were compared with the methyl-substituted analogues, crotonaldehyde **1a** and tiglic aldehyde **1i**. In both the latter cases, the β-substituted enals reacted significantly faster with $BnNH_2$ **2a** and $PhNH_2$ **2b**. Remarkably, the reaction between cinnamaldehyde **1g** and $BnNH_2$ **2a** was complete in <10 minutes, with 50% being consumed in approximately 1 minute, as shown in the three superimposed IR-spectra at t = 0, 1 and 9 min in Figure 6.

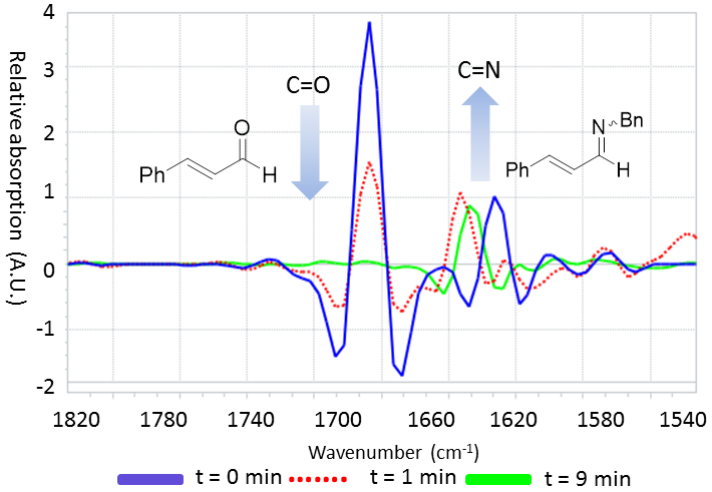

Figure 6 Superimposed IR spectra at t = 0, t = 1, t = 9 min, showing the loss of **1g** (C=O, 1685 cm^{-1}) and the shift of the C=C in **1g** (from 1630 to 1644 cm^{-1}) on the addition of **2a.** The concomitant gain of the product C=N **3ga** stretch (1641 cm^{-1}) can be observed (Entry 2, Table 6). Processing - 2nd derivative base-line function is applied.

Table 6 Probing substituent effects of enals and enones.

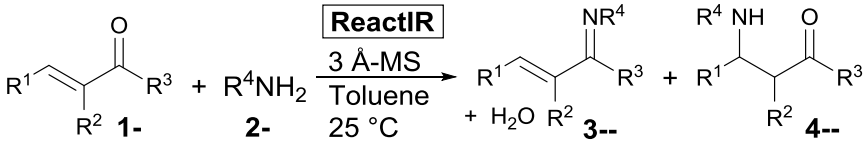

Entry	Substrate **1-**	Amine **2-**	Primary Product	Time, t (min)	$I_{C=O\ 1/2}$ (min)
1	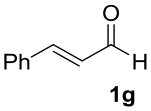 **1g**	$PhNH_2$ **2b**	**3gb**	78	7
2		$BnNH_2$ **2a**	**3ga**	9	1
3	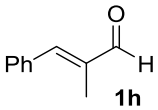 **1h**	$PhNH_2$ **2b**	**3hb**	220	25
4		$BnNH_2$ **2a**	**3ha**	202	24
5	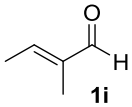 **1i**	$PhNH_2$ **2b**	**3ib**	545	28
6		$BnNH_2$ **2a**	**3ia**	233	29
7	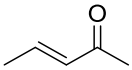 **1j**	$PhNH_2$ **2b**	**3jb**	>1440	-[a]
8		$BnNH_2$ **2a**	**3ja**	>1440	165
9	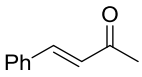 **1k**	$PhNH_2$ **2b**	**3kb**	>1440	139
10		$BnNH_2$ **2a**	**3ka**	>1440	115
11	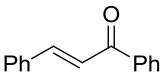 **1l**	$PhNH_2$ **2b**	**3lb**	>1440	517
12		$BnNH_2$ **2a**	**3la**	>1440	108

Conditions: Enone/enal **1** (2 mmol) was added to a 25 ºC stirred toluene (8 mL) suspension of 3 Å-MS beads (oven-dried at 250 ºC for >48 h prior to use). Amine **2** (2 mmol) was added and the reaction monitored by ReactIR™. [a]Peak intensity = 55% after 24 h.

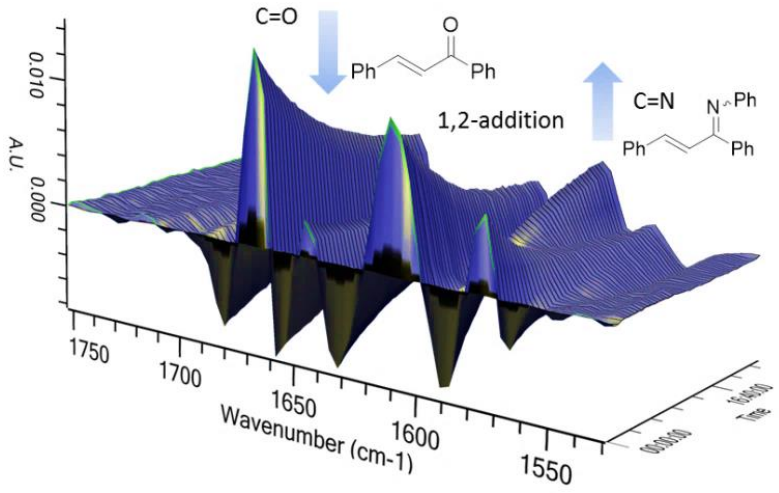

Figure 7 Graphical output of entry 11, Table 6. Addition of **2b** to **1l** results in the slow formation of **3lb**, but no 1,4-addition products are observed. Processing - 2nd derivative base-line function is applied.

Theoretical study of the selectivity in amine addition to α,β-unsaturated aldehydes and ketones

In order to understand the origin of the observed selectivity in the addition of amines to the enals and enones, DFT calculations (B3LYP functional) were carried out on representative substrates (*i.e.* crotonaldehyde **1a**, methyl vinyl ketone **1c**, cyclopentenone **1d** and pentenone **1j**) using $MeNH_2$ as a model of a simple primary alkylamine. These calculations indicated that the kinetic preference for the 1,2- *vs.* 1,4-addition pathway depends on the conformational effects operating upon the α,β-unsaturated aldehydes and ketones. When the C=C and C=O bonds are *s-trans* to each other, the 1,2-addition pathway shows lower energy barriers and in contrast, when they are *s-cis*, the 1,4-addition pathway is preferred (see Table 7 and ESI for additional comments). Indeed, one should note literature examples which suggest that the stereochemistry involved in the addition of crotyl magnesium chloride to enones is also notably dependent upon the enone conformation.[14]

Table 7 NBO orbital energies of $\pi^*_{C=O}$ and $\pi^*_{C=C}$ (in eV); and energy barriers ($\Delta E^{\neq}$ in kcal.mol^{-1}) for the 1,2- and 1,4-addition of $NMeH_2$ to α,β-unsaturated aldehydes and ketones; and NBO second-order perturbative donor-acceptor interaction between the C_α lone pair and the $\pi^*_{C=O}$ orbital at the transition state for 1,4-addition (kcal.mol^{-1}).

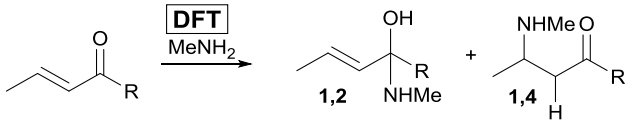

	$\pi^*_{C=O}$	$\Delta E^{\neq}$(1,2)	$\pi^*_{C=C}$	$\Delta E^{\neq}$(1,4)	$n_{C\alpha}\rightarrow\pi^*_{C=C}$	$\Delta\Delta E^{\neq}$
1a *s-trans*	**0.42**	**33.0**	**0.82**	**37.4**	**64**	**+4.4**
s-cis	0.41	30.3	1.10	29.0	76	-1.3
1c *s-trans*	0.57	35.5	0.86	37.4	68	+1.9
s-cis	**0.63**	**33.4**	**0.98**	**27.1**	**75**	**-6.3**
1j *s-trans*	0.74	36.6	1.18	40.1	70	+3.5
s-cis	**0.78**	**34.6**	**1.30**	**30.4**	**75**	**-4.2**
1d *s-trans*	**0.80**	**38.2**	**1.02**	**38.9**	**65**	**+0.7**

The predominance for 1,2- over 1,4-addition in the *s-trans* conformation can be explained from the relative energy of the acceptor π*-orbitals.[15] The origin of this effect is due to the fact that energies of the $\pi^*_{C=O}$ orbitals are lower than those of the $\pi^*_{C=C}$ orbitals, suggesting that the electrophilic carbon of the carbonyl group is more reactive than that of the C=C double bond in the *s-trans* conformation. Indeed, for *s-trans* conformers, a linear correlation between the computed energy barriers and the energies of the $\pi^*_{C=O}$ and $\pi^*_{C=C}$

orbitals was observed (see Figure 8). In contrast, when *s-cis* conformers are considered, no correlation between the activation barriers and the energies of the π-antibonding orbitals is observed.

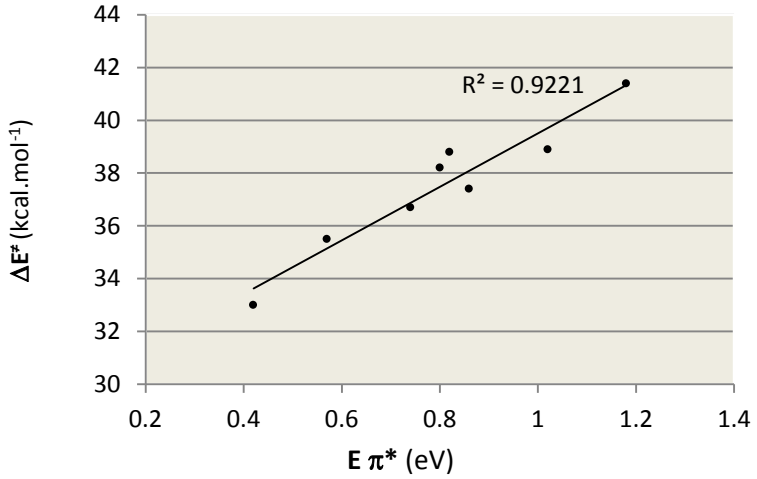

Figure 8. Correlation between the computed energy barriers and the energies of the C=C and C=O π* orbitals in the *s-trans* isomers.

In the *s-cis* conformation, the energy barriers for 1,4-addition pathway ($\Delta E^{\neq}(1,4)$) are lowered significantly (~10 kcal.mol^{-1}), with respect to those of the *s-trans* forms (see Table 7). Analogously, calculations have shown that the *s-cis* conformation of α,β-unsaturated aldehydes is more reactive towards the addition of dienes.[16] Houk *et al.* attributed the larger reactivity to the greater electrophilicity of the *s-cis* conformer and also suggested that secondary orbital interactions between the carbonyl and the diene play a key role in controlling stereoselectivity.[16b] Herein, the NBO analysis shows that the reactivity is not consistent with the lower energy of the $\pi^*_{C=C}$ orbitals. Instead, we find a clear correlation with a greater intramolecular $n(C_\alpha) \rightarrow \pi^*_{C=O}$ interaction in the transition state (see Table 7). The developing negative charge at the α-carbon is better delocalized through the $\pi^*_{C=O}$ orbitals when the C=O and (reacting) C=C bonds are *s-cis*. For example, in the 1,4-addition

TS of methyl vinyl ketone **1c**, the NBO n(C_α) → $\pi^*_{C=O}$ interaction energies (68 and 75 kcal.mol^{-1}) correlate with energy barriers of 37.4 and 27.1 kcal.mol^{-1} for *s-trans* and *s-cis*, respectively. Indeed, the HOMO of the transition states have a strong contribution *via* this interaction, that is, a bonding combination of the p-orbitals of the α-C-atom and the π* orbitals of C=O moiety (see Figure 9). It is important to note that in this TS, the axis of the forming C-H bond is bent towards the C=O moiety in an *s-cis* form, whereas, it is bent towards the C(O)-Me in the *s-trans* form, generating two different stereo-configurations (see Figure 12 in ESI). In summary, the different balance between electronic effects on going from the *s-trans* to the *s-cis* conformers results in reversing the relative reactivity of the C=C and C=O functional groups.

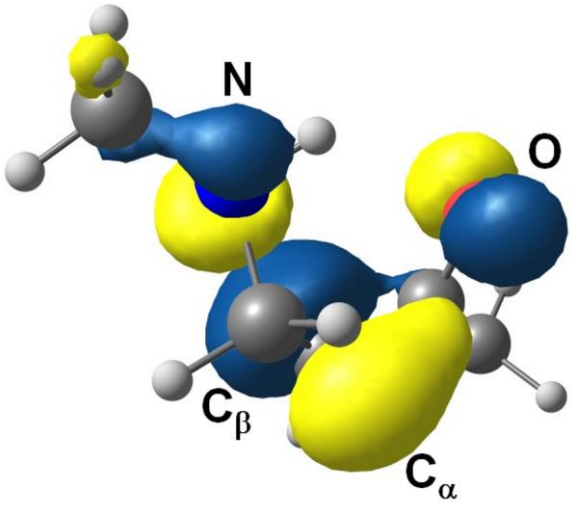

Figure 9. Representation of the $p_{C\alpha}$-$\pi^*_{C=O}$ interaction in the HOMO orbital for the transition state of the 1,4-addition in the *s-cis* isomer of **1c**.

For crotonaldehyde **1a**, the *s-trans* conformation is thermodynamically favoured over the *s-cis* conformation by 1.3 kcal.mol^{-1}, thereby selectively leading to the kinetically preferred 1,2-addition imine product **3**. Our computed relative stabilities agree with the results of the high-level calculations[17] and experiments,[18] in which the *s-trans* conformers are favored by 2.1 and 1.7 kcal.mol^{-1}, respectively. In addition, vibrational spectroscopic studies

showed that only the *s-cis* conformation exists in solution,[18] indicating that only the *s-trans* reaction pathway is operative. For the aliphatic ketones **1c** and **1j**, the additional alkyl group most likely induces steric repulsion with the double bond, destabilizing the *s-trans* conformer which results in shifting the equilibrium towards the *s-cis* conformer, and in turn this is more stable by 0.3 and 0.7 kcal.mol^{-1}, respectively for **1c** and **1j**. In the case of **1c**, spectroscopic studies revealed that both the *s-cis* and *s-trans* conformations existed,[19] with the energy difference between them reduced to less than 1 kcal.mol^{-1}.[19b] Thus, the reaction is likely to proceed through the lowest energy transition states available and that means the *s-cis* pathway. These systems of course, contrast with the cyclic enones. Since they can only adopt the *s-trans* conformation, the kineticically preferred reaction pathway becomes the 1,2-addition process. Although the energy difference for cyclopentenone **1d** is quite small, it follows the same trend as the other *s-trans* conformer substrates.

Comparing the different substrates, it was observed that the computed overall energy barriers for the preferred reaction pathways follow the order: aliphatic ketone < aldehydes < cyclic ketones. This is in line with experimental results and supports the idea that the nucleophilic amine addition is the rate-determining step under these non-acidic conditions. As expected, and in all cases, the 1,4-products are thermodynamically favoured over the hemi-aminal intermediates resulting from the 1,2-addition mode (see ESI). Thus, not only is the 1,2-addition product kinetically controlled, but also, the 1,4-addition product is observed for methyl vinyl ketone **1c**, which is kinetically preferred as a direct consequence of the conformation change that occurs.

Upon expanding the scope of the substrates examined by the DFT calculations, we were surprised to find that the other linear enones prefer to give the 1,2-addition products (*i.e.* **1j**, **1k** and **1l** in Table 6). This supports the results obtained from the ReactIR and *in situ* ^{1}H-NMR studies (*vide supra* and ESI). Following on from **1c** to **1j**, the calculated barriers

showed the same pattern as previously identified, however, for the 1,4-addition to C=C, they were found to be somewhat higher for **1j** (*i.e.* by around 3 kcal.mol^{-1}) than **1c**, as expected for a substrate with an electron-donating substituent on the C=C (**1j**).

Summary and conclusions

The relative reactivity of enones and enals with primary amines has been examined, probing the competitive 1,2- *vs.* 1,4-addition pathway using a combination of *in situ* IR spectroscopy (ReactIR), *in situ* NMR and DFT calculations. The *in situ* IR spectroscopy (ReactIR) revealed that enones and enals undergo either 1,2-(to C=O) or 1,4-addition (to C=C) with primary amines (with or without 3 Å-MSs). This suggested that the formation of α,β-unsaturated imines (formed through 1,2-addition to C=O) is under kinetic control for all enals and most enones. However, compounds such as methyl vinyl ketone showed exclusive 1,4-addition, suggesting that 1,4-addition products (*i.e.* β-amino ketones) are kinetically favoured in this case. ReactIR investigations conducted in parallel with a series of *in situ* ^{1}H-NMR experiments allowed us to confirm the validity of the observations made by ReactIR, with the exception of pentenone **1j** which showed slow and competing 1,2- *vs.* 1,4-addition (see ESI). *In situ* methods for the analysis of such substrates and reactions is advantageous due to avoiding facile hydrolysis, polymerization and degradation of the sensitive product α,β-unsaturated imines.[20] These problems make isolation of the α,β-unsaturated imines problematic and hence this highlights the advantages of forming them *in situ* for subsequent transformations. Since ReactIR is a relatively non-invasive method with measurements made *in situ* without causing degradation of air or moisture sensitive intermediates, as exemplified by its use in monitoring low-temperature lithiations.[21]

Stimulated by the data acquired by our ReactIR studies, we turned our attention to seeking theoretical explanations for the observed results. DFT calculations were carried out

which indicate that the selectivities in these addition reactions are governed by conformational and stereoelectonic effects, whereby *s-trans* conformations kinetically favor 1,2-additions and *s-cis* conformations kinetically favor 1,4–additions. Moreover, substitution effects can cause conformational swap-over due to these steric effects.

The rationalization of the interplaying effects involved in preparing unsaturated imines from unsaturated ketones and aldehydes makes the preparation and utilization of the resulting α,β-unsaturated imines *in situ* more predictable. The clean and selective formation of such imines *in situ* has already proven valuable our hands for reacting with boryl nucleophiles,[2] and it is expected that these results offer the potential for wider applications in synthesis.

Experimental Section

General Experimental

All *in situ* IR spectroscopy experiments (ReactIR) were carried out on the following instrument: ReactIR 15 with MCT detector; ConcIRT window = 1900-900 cm^{-1}. Apodization = Happ General. Probe: Prob A DiComp (Diamond) connected *via* KAgX 9.5 mm x 2m Fiber (Silver Halide); Sampling 2500-650 at 8 cm^{-1} resolution; Scan option: auto select, gain 1X. ^{1}H NMR spectra were recorded on a Varian-Mercury 500 MHz spectrometer, operating at ambient probe temperature unless specified elsewhere. Deuterated toluene (d8-toluene) was used as solvent for all NMR spectra, unless specified elsewhere.

Standard conditions for ReactIR experiments

To an oven-dried two-necked flask, fitted with the IR probe (see above), **1** (2.0 mmol) was added to a stirring solution of toluene (8.0 mL) and 3 Å-molecular sieve beads (2.0 g, oven-

dried at 250 ºC for >48 h prior to use), under Ar at 25 ºC. Once the C=O peak had plateaued, showing maximum intensity, amine **2** (2.0 mmol) was added and the reaction was carried out for 0.5 – 24 h.

Standard conditions for *in situ* ^{1}H-NMR experiments

Enal or enone **1** (0.18 mmol) was added to an NMR tube (Norell® Standard Series™ 5 mm x 178 mm NMR tubes) containing d8-toluene (0.7 mL) with/without 3 Å-MS beads (filled 0.7-0.8 mm up the tube, MS beads oven-dried at 250 ºC for >48 h prior to use), and flushed with Argon and sealed. One the acquisition of the first spectrum, amine **2** (0.18 mmol) was added and the next spectrum was acquired in <5 min. Subsequent ^{1}H-NMR spectra were recorded over time with intermittent shaking of the NMR tube to aid mixing (see ESI).

Computational details

All calculations were performed using the Gaussian09 series of programs.[22] Full quantum mechanics calculations on model systems were performed within the framework of density functional theory (DFT) using the B3LYP functional.[23] The basis set for all the atoms was the 6-31G(d,p).[24] All geometry optimizations were full, with no restrictions using the Berny algorithm implemented in Gaussian09.[25] All minima and transition states were confirmed by performing frequency calculations. Transition states were characterized by single imaginary frequency, whose normal mode corresponded to the expected motion. Since the qualitative trends on selectivity are not affected by the polarity of the solvent (see Tables 2 and 3), calculations were performed in vacuum. The natural bond orbital (NBO) method[26] was used to analyze the resultant wave function in terms of optimally chosen localized orbitals, localized orbitals corresponding to a Lewis structure representation of chemical bonding. In the case of some *s-cis* transition states, the optimal Lewis structure was slightly modified to

account for the second-order perturbative donor-acceptor interaction between the C_α lone pair and the $\pi^*_{C=O}$ orbital.

Acknowledgments

We thank the EPSRC for Doctoral Training Account funding to A. D. J. C. and the Ministerio de Ciencia e Innovación (MICINN) of Spain (project CTQ2011-29054-C02-01 and CTQ2010-16226) and from the Direcció General de Recerca (DGR) of the Autonomous Government of Catalonia (grants 2009SGR462 and XRQTC).

References

1. a) Perlmutter, P. *Conjugate Addition Reactions in Organic Synthesis*, Tetrahedron Organic Chemistry, Pergamon, Oxford, 7th edn, **1992**; b) Rossiter, B. E.; Swingle, N. M. *Chem. Rev.*, **1992**, *92*, 771; c) Csáky, A. G.; de la Herrán, G.; Murcia, M. C. *Chem. Soc. Rev.*, **2010**, *39*, 4080.
2. For our previous work regarding the utilization of α,β-unsaturated imines in synthesis, see: a) Fernández, E.; Gulyás, H.; Solé, C.; Whiting, A. *Adv. Synth. Catal.*, **2011**, *353*, 376.; b) Fernández, E.; Gulyás, H.; Solé, C.; Mata, J. A.; Tatla, A.; Whiting, A. *Chem.–Eur. J.*, **2011**, *17*, 14248.; c) Calow, A. D. J.; Batsanov, A. S.; Fernández, E.; Solé, C.; Whiting, A. *Chem. Commun.*, **2012**, *48*, 11401.; d) Calow, A. D. J.; Solé, C.; Whiting, A.; Fernández, E. *ChemCatChem*, **2013**, *5*, 2233.; e) Calow, A. D. J.; Batsanov, A.; Pujol, A.; Solé, C.; Fernández, E.; Whiting, A. *Org. Lett.*, **2013**, *15*, 4810.
3. a) Osman, R.; Pardo, L.; Rabinowitz, J. R.; Weinstein, H. *J. Am. Chem. Soc.*, **1993**, *115*, 8263.; b) Blackmond, D. G.; Hii, K. K.; Mathew, S. P.; Phua, P. H.; White, A. J. P.; de Vries, J. G. *Chem. Eur. J.*, **2007**, *13*, 4602.; c) Bernasconi, C. F. *Tetrahedron.*, **1989**, *45*, 4017.

4. a) Hine, J.; Via, F. A. *J. Am. Chem. Soc.*, **1972**, *94*, 190.; b) Hine, J.; Craig Jr., J. C.; Underwood II, J. G.; Via, F. A. *J. Am. Chem. Soc.*, **1970**, *92*, 5194.; c) Chou, Y.; Hine, J. *J. Org. Chem.*, **1981**, *46*, 649.; d) Available online: Ian. J. Smith, PhD Thesis, Durham University, **2003**; e) Atherton, J. H.; Brown, K. H.; Crampton, M. R., *J. Chem. Soc., Perkin Trans. 2.*, **2000**, *5*, 941.; f) Sayer, J. M.; Jencks, W. P. *J. Am. Chem. Soc.*, **1977**, *99*, 464.; g) Hoffman, R. V.; Bartsch, R. A.; Rae Cho, B. *Acc. Chem. Res.*, **1989**, *22*, 211.
5. a) Ellman, J. A.; McMahon, J. P. *Org. Lett.*, **2005**, *7*, 5393.; b) Bergman, R. G.; Colby, D. A.; Ellman, J. A. *J. Am. Chem. Soc*., **2006**, *128*, 5604.; c) Bergman, R. G.; Colby, D. A.; Ellman, J. A. *J. Am. Chem. Soc*., **2008**, *130*, 3645.
6. a) Cossío, F. P.; Odriozola, J. M.; Oiarbide, M.; Palomo, C. *J. Chem. Soc., Chem. Commun.***, 1989**, 74.; b) Dembkowski, L.; Ganboa, I.; Kot, A.; Palomo, C. *J. Org. Chem*., **1998**, *63*, 6398.; c) Aizpurua, J. M.; Ganboa, I.; Oiarbide, M.; Palomo, C. *Eur. J. Org. Chem*., **1999**, 3223.
7. Arndtsen, B. A.; Lu, Y. *Org. Lett.*, **2009**, *11*, 1369.
8. a) Aparicio, D.; Palacious, F.; Vicario, J. *J. Org. Chem.*, **2006**, *71*, 7690.; b) Palacios, F.; Pascual, S.; Ochoa de Retana, A. M.; Fernández de Trocóniz, G. *Tetrahedron.*, **2011**, *67*, 1575.; c) Ezpeleta, J. M.; Palacious, F.; Pascual, S.; Ochoa de Retana, A. M.; Fernández de Trocóniz, G. *Eur. J. Org. Chem.*, **2013**, 5614.
9. Alonso, C.; Ayerbe, M.; Cossío, F. P.; Lecea, B.; Palacios, F.; Rubiales, G. *J. Org. Chem.*, **2006**, 71, 2839.
10. a) Moyer, S. A.; Pearce, S. D.; Rigoli, J. W.; Schomaker, J. M. *Org. Biomol. Chem.*, **2012**, *10*, 1746.; b) Soulé, J.-F.; Miyamura, H.; Kobayashi, S. *Chem. Commun.*, **2013**, *49*, 355.

11. Carter, C. F.; Lange, H.; Ley, S. V.; Baxendale, I. R.; Wittkamp, B.; Goode, J. G.; Gaunt, N. L.; *Org. Process Res. Dev.*, **2010**, *14*, 393.

12. For information regarding additions to enones under kinetic or thermodynamic control, see: Schultz, A. G.; Yee, Y. K. *J. Org. Chem.*, **1976**, *41*, 4044.

13. Available online: Kathryn H. Brown, PhD Thesis, Durham University, **1999.**

14. a) Benhallam, R.; Zair, T.; Jarid, A.; Ibrahim-Ouali, M.; *J. Mol. Struct. (THEOCHEM)*, **2003**, *626*, 1; b) Benhallam, R.; Essaoudi, A.; Zair, T.; *Phys. & Chem. News*, **2002**, *8*, 110.

15. See for example: Romo, S.; Antonova, N. S.; Carbó, J. J.; Poblet, J. M. *Dalton Trans.*, **2008**¸ 5166.

16. a) Barba, C.; Carmona, D.; García, J. I.; Lamata, M. P.; Mayoral, J. A.; Salvatella, L.; Viguri, F.; *J. Org. Chem.*, **2006**, *71*, 9831; b) Loncharich, R. J.; Brown, F. K.; Houk, K. N.; *J. Org. Chem.* **1989**, *54*, 1129.

17. Bokareva, O. S.; Bataev, V. A.; Godunov, I. A.; *J. Mol. Struct. (THEOCHEM)*, **2009**, *913*, 254.

18. Durig, J. R.; Brown, S. C.; Kalasinsky, V. F.; George, W. O.; *Spectrochim. Acta A*, **1976,** *32*, 807.

19. a) Fantoni, A. C.; Caminati, W.; *Chem. Phys. Lett.*, **1987**, *133*, 27; b) During, J. R.; Little, T. S.; *J. Chem. Phys.*, **1981**, *75*, 3660; c) Krantz, A.; *J. Am. Chem. Soc.*, **1972**, *94*, 4022.

20. Feringa, B. L.; Jansen, J. F. G. A.; *Synthesis*., **1988**, *3*, 184.

21. See example of ReactIR being used to follow a low-temperature lithiations:
Campos, K. R.; Carbone, G.; Coldham, I.; O'Brien, P.;Sanderson, A.; Stead, D. *J. Am. Chem. Soc.*, **2010**, *132*, 7260.

22. Gaussian09 (Revision A.02): Frisch, M. J.; Trucks, G. W.; Schlegel, H. B.; Scuseria, G. E.; Robb, M. A.; Cheeseman, J. R.; Scalmani, G.; Barone, V.; Mennucci, B.; Petersson,

G. A.; Nakatsuji, H.; Caricato, M.; Li, X.; Hratchian, H. P.; Izmaylov, A. F.; Bloino, J.; Zheng, G.; Sonnenberg, J. L.; Hada, M.; Ehara, M.; Toyota, K.; Fukuda, R.; Hasegawa, J.; Ishida, M.; Nakajima, T.; Honda, Y.; Kitao, O.; Nakai, H.; Vreven, T.; Montgomery Jr., J. A.; Peralta, J. E.; Ogliaro, F.; Bearpark, M.; Heyd, J. J.; Brothers, E.; Kudin, K. N.; Staroverov, V. N.; Kobayashi, R.; Normand, J.; Raghavachari, K.; Rendell, A.; Burant, J. C.; Iyengar, S. S.; Tomasi, J.; Cossi, M.; Rega, N.; Millam, J. M.; Klene, M.; Knox, J. E.; Cross, J. B.; Bakken, V.; Adamo, C.; Jaramillo, J.; Gomperts, R.; Stratmann, R. E.; Yazyev, O.; Austin, A. J.; Cammi, R.; Pomelli, C.; Ochterski, J. W.; Martin, R. L.; Morokuma, K.; Zakrzewski, V. G.; Voth, G. A.; Salvador, P.; Dannenberg, J. J.; Dapprich, S.; Daniels, A. D.; Farkas, O.; Foresman, J. B.; Ortiz, J. V.; Cioslowski, J.; Fox, D. J. Gaussian, Inc., Wallingford CT, 2009.

23. a) Lee, C.; Yang, W.; Parr, R. G. *Phys. Rev. B* **1988**, *37*, 785.; b) Becke, A. D. *J. Chem. Phys.* **1993**, *98*, 5648.; c) Stephens, P. J.; Devlin, F. J.; Chabalowski, C. F.; Frisch, M. J.; *J. Phys. Chem.* **1994**, *98*, 11623.
24. a) Francl, M. M.; Pietro, W. J.; Hehre, W. J.; Binkley, J. S.; Gordon, M. S.; Defrees, D. J.; Pople, J. A. *J. Chem. Phys.* **1982,** *77*, 3654.; b) Hehre, W. J.; Ditchfield, R.; Pople, J. A. *J. Chem. Phys.*, **1972,** *56*, 2257.; c) Hariharan, P. C.; Pople, J. A. *Theor. Chim. Acta* **1973,** *28*, 213.
25. Pulay, P.; Fogarasi, G.; *J. Chem. Phys.* **1992**, *96*, 2856
26. Reed, A. E.; Curtiss, L. A.; Weinhold, F. *Chem. Rev.* **1988**, *88*, 889.